Periodica Polytechnica Transportation Engineering, 53(2), pp. 194–205, 2025

Investigation of Turbojet Engine Performance in Subsonic Flight Conditions with Turbofan Power Ratio as Thrust Parameter

Khaoula Derbel[1], Károly Beneda[1*]

[1] Department of Aeronautics and Naval Architecture, Faculty of Transportation Engineering and Vehicle Engineering, Budapest University of Technology and Economics, H-1111 Budapest, Műegyetem rkp. 3., Hungary
[*] Corresponding author, e-mail: karoly.beneda@kjk.bme.hu

Received: 28 May 2024, Accepted: 20 February 2025, Published online: 24 March 2025

Abstract

Turbojet engines have been used for many decades in aviation. Although their share in civil aviation is minimal, with the advent of Unmanned Aerial Vehicles (UAV's) there are new applications. Their operation depends on complex aero-thermodynamic laws, and optimum performance is strongly affected by the control system. The authors have previously investigated how the Turbofan Power Ratio (TPR), originally introduced on Rolls-Royce commercial turbofans, can be used in control of single stream turbojet engines. Based on those results, in the present paper the assessment of flight characteristics is introduced, based on mathematical models, which are available of the particular gas turbine type under investigation. Like the corrected rotor speed, the ratio of TPR and actual thrust depends on Mach number, therefore, this function is determined in this paper. The investigations also included a deteriorated model under control of both corrected rotor speed and TPR, which has shown that TPR can partially recover thrust loss thus improving the safety of the power plant. As a conclusion, TPR is worth of utilizing in control systems as it results in more straightforward thrust correlation and reduced performance loss over time. Furthermore, measuring simultaneously with other common engine parameters, the extent of deterioration can be signalized to the crew before it evolves into a catastrophic failure.

Keywords

turbojet, Turbofan Power Ratio, engine flight characteristics, engine deterioration, powerplant diagnostics

1 Introduction

The goal of this paper is to perform an investigation of Turbofan Power Ratio (TPR), to identify its applicability as thrust parameter for single stream turbojet engines under subsonic flight conditions. This compound parameter was introduced by Rolls-Royce originally (Davies et al., 2006) and can be seen in Eq. (1), with p_{t2} and p_{t3} being the inlet and outlet total pressures of the compressor, respectively, T_{t2} is compressor inlet total temperature, and T_{t5} is turbine discharge total temperature:

$$\mathrm{TPR} = \frac{p_{t3}}{p_{t2}} \sqrt{\frac{T_{t5}}{T_{t2}}}. \tag{1}$$

The rest of Section 1 details the actuality of the work by introducing turbojet engines and their possible control. Section 2 introduces the component level mathematical model, which is used in the present assessment. The model has two branches, one for the baseline (nominal, undeteriorated) compressor and another for the deteriorated case, which has the role to investigate the effects of compressor degradation on the operation of the power plant. Section 3 begins with the verification of the model, then it contains a description of Mach number dependency of TPR-to-thrust ratio, which is a new achievement of this paper, finally it shows details of effect of TPR control on the engine behavior with deteriorated compressor. Connecting to the previous thoughts, Section 4 provides further discussion on the achieved results. Finally, Section 5 provides a conclusion for the paper.

1.1 Turbojet engines

Turbojet engines were among the first operational gas turbines for aircraft propulsion, which revolutionized air transport in the mid-20th century. They allowed significant increase in velocity, which allowed for shortening flight durations, reaching longer ranges and higher altitudes. However, their operation was not optimal in the speed range

Cite this article as: Derbel, K., Beneda, K. (2025) "Investigation of Turbojet Engine Performance in Subsonic Flight Conditions with Turbofan Power Ratio as Thrust Parameter", Periodica Polytechnica Transportation Engineering, 53(2), pp. 194–205. https://doi.org/10.3311/PPtr.37560

dictated by commercial flight. Although there were plans to develop a supersonic transport aircraft in all major design bureaus, due to changing economic circumstances, finally only two types reached production and British Aircraft Corporation (BAC)-Aerospatiale Concorde was the only one operated for a considerable period. As commercial aviation abandoned the plans for supersonic flight, the improvement of gas turbine engines took a different path, and first low, then high bypass ratio turbofan engines evolved. These offer significantly lower thrust specific fuel consumption and have superseded single stream turbojet engines almost totally. However, few utilizations are still possible, mostly in military applications, where high velocity is not a limiting factor, and very often they provide propulsion for Unmanned Aerial Vehicles (UAV's) (Yucer and Nacakli, 2024). This still new and constantly emerging segment of aviation has opened new aspects of turbojets as well, where simplicity weighs more than other aspects in which turbofans or turboprop engines would otherwise dominate. Consequently, even if this segment is limited, there are surely operators, where these engines will be maintained in service for additional decades in the future, thus, it is worth carrying out investigations to improve the efficiency and reliability of turbojet engines. A few examples of current research topics involving turbojets include the development of robust, adaptive (Főző et al., 2019) or fault tolerant controls (Han, 2023), self-tuning proportional-integral-derivative (PID) systems (Gao et al., 2024), or may focus particularly on less deeply discovered transient phenomena like effects of starting fuel scheduling and its possibilities of improvement (Montazeri-Gh and Dastjerdi, 2024). Furthermore, there is a strong demand of creating engines capable of running on hydrogen, thus a lot of engineering challenges are found in combustion related fields like effects of pure hydrogen supply (Balli, 2022) or combined fuel injection systems with simultaneous supply of Jet A1 and hydrogen (Brodzik, 2024), environmental impacts of using hydrogen as power source including exergy analysis (Yucer and Nacakli, 2024) or focusing on pollution particles (Ciupek et al., 2024). There are some researches that deal with the problems of the combination of hydrogen fuel and traditional control systems (Xiao et al., 2023). Other bio- and sustainable aviation fuel blends are also in focus as reported by Şen (2023) or more common liquids like ethanol (Andoga et al., 2021). Investigation of methods that are suitable for any turbine engine are also quite often performed on simple, less expensive turbojets, like noise reduction with chevrons (Cican et al., 2023), development of optimal temperature distribution at the turbine inlet for reduction of blade and vane distress (Ghahramani et al., 2023), optimization of pressure ratio (Zare and Veress, 2022) or multi-objective optimization with genetic algorithms, particle swarm or grey wolf methods (Aygun et al., 2023), health monitoring of bearings (Przysowa et al., 2023), exergy analysis (Balli et al., 2022) or endoscopic particle image velocimetry (PIV) methods (Rohacs et al., 2023). There are also novel approaches, which can be used in more electric aircraft like electrically driven fuel-oil pumps and their advanced control (Főző and Andoga, 2022) or intelligent thermal imaging dedicated to diagnostic functions of turbojet engine operation (Andoga et al, 2019).

Turbojets belong to the group of gas turbines, which produce thrust for propulsion. They can have one or more (typically two, maximum three) rotating assemblies, each equipped with a compressor unit (of one or multiple stages, which are of axial and/or centrifugal ones) that supplies an increasing pressure of air towards a combustion chamber, where fuel is constantly burned with incoming pressurized air during the operation, and a turbine unit (with one or more stages, mostly axial, sometimes radial ones) downstream of the combustor that is mounted to the same shaft and produces the drive torque for its own compressor. The exhaust gas has considerable energy content; thus, they can be used in a nozzle to produce thrust output. A typical turbojet engine is shown in Fig. 1, which is a simplified schematic of the engine under investigation. Some numbers are not included in the list of aerodynamic stations, as they represent such cross-sections of the engine, which are not realized in all designs, like afterburning, throat of a converging-diverging nozzle, etc.

1.2 Control of turbojet engines

Considering the engine as a machine that converts energy, one can state that it takes place in two major steps:

1. the chemical energy contained within the fuel is turned into heat energy in the combustion chamber,

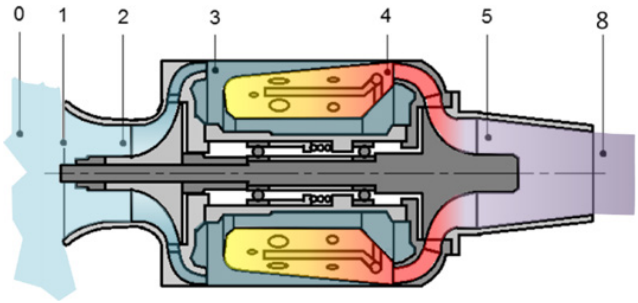

Fig. 1 Simplified longitudinal section of a simple turbojet engine with designation of major aerodynamic stations

2. the heat energy is then converted into kinetic energy of the exhaust gas to accelerate it in contrast to that state in which it has entered the engine.

Control of turbojet engines has the goal to maintain a desired thrust set by either the flight crew or an auto flight system. However, although there were investigations to overcome this limitation, thrust cannot normally be measured when the engine is installed on an aircraft, because several other forces are occurring, and the net force cannot be separated from other individually unknown components, only an aggregate value could be determined. Therefore, engine control systems are based on parameters of the turbojet, which show proportionality with the net thrust component. The most widely used parameters are the following:

- Rotor speed (in case of multiple rotors, the designer may choose any one which has more suitable behavior for the given operation): this parameter strongly affects the amount of air that is drawn into the engine and the pressures throughout the flow path, thus proportionality is provided, but it is far not linear. Furthermore, ambient conditions also influence the actual thrust output at a given rotor speed, thus, if the aircraft has a considerable speed range (even in commercial subsonic aviation), the engine control system must incorporate shifting of the control line due to these changing operating circumstances. Nevertheless, a considerable percentage of the gas turbine engines are controlled by rotor speed, and recent researches also focus on the improvement of this method e.g., (Tang et al., 2020).
- Engine Pressure Ratio (EPR), which is the ratio of pressures at the turbine discharge and the compressor inlet, typically measured as total values (not static): this ratio expresses how much the working medium will be accelerated in the exhaust nozzle but excludes ram effect up to the intake of the engine. This offers less nonlinearity in contrast to rotor speed and is therefore more closely proportional to the main parameter, thrust (Arif et al., 2018).
- TPR: this parameter was developed by Rolls-Royce and was used in their commercial turbofan engines as reported by a conference paper (Davies et al., 2006) or as it is shown in a patent (Rowe and Kurz, 1999). Although not being a parameter originally dedicated to turbojet engines, investigating its definition in Eq. (1) it can be stated that it does not contain any specific parameter, which only holds for turbofans but cannot be implemented in a turbojet.

Although originally the definition of TPR contained turbine inlet temperature T_{t4} in the numerator of the square root ratio, Rowe and Kurz (1999) already suggest utilization of T_{t5} in their original patent due to difficulties in measurement of T_{t4}. The authors have also used turbine exhaust gas temperature T_{t5} in the present investigation.

The authors have previously carried out several studies regarding the possibility of utilization of TPR in the control system of turbojet engines. It was proven that the parameter itself can be used as thrust parameter (Beneda, 2015), and in case of a constant flight condition (altitude and velocity kept unchanged), TPR shows a linear correlation with thrust. Several measurements have also been performed, which demonstrate this correlation.

A complete modular electronic control system was built that implemented a PID algorithm for TPR control. Accuracy of reference tracking was very good according to the measurements carried out.

Later, a Linear Quadratic Integrator control was designed (Derbel and Beneda, 2019), and a Sliding Mode Control has been investigated as well (Derbel and Beneda, 2020). The latter showed superior characteristics against conventional control algorithms.

After several successful ground tests, a flight measurement was prepared. The present paper is connected to this, its goal is to establish the theoretical background of the relationship between TPR, and engine thrust when the engine is installed on an aircraft and flight conditions can change significantly.

2 Mathematical model of the turbojet engine under changing flight conditions

The mathematical model, which can be used to determine the behaviour of the turbojet engine within a wide range of flight conditions (altitude, Mach number), is necessarily built on a non-linear basis to consider those effects are inherent to all gas turbines. This includes component characteristics and general gas dynamic correlations as well. In the latter aspect, air and gas parameters are calculated as a function of temperature and gas composition. This requires an iteration in compressor, turbine and exhaust nozzle as the flow parameters implicitly contain either specific heat at constant pressure or the adiabatic exponent. In Subsections 2.1 to 2.5, the component level models are introduced.

2.1 Atmosphere and air intake duct

As turbojet engines are intended for flights basically in lower altitudes, mostly tropospheric conditions, the Inter-

national Standard Atmosphere (ISA) is used to calculate ambient conditions. The model has the possibility to incorporate deviations in both temperature (ΔT_{std}) and pressure (Δp_{std}) at the sea level, thus real-day conditions can be calculated besides the standard nominal circumstances, according to Eqs. (2) and (3), where the sea level standard day values are $T_{0,H=0} = 288$ K and $p_{0,H=0} = 101{,}325$ Pa, respectively:

$$T_{0,H} = T_{0,H=0} - 0.0065H + \Delta T_{std}, \tag{2}$$

$$p_{0,H} = p_{0,H=0}\left(\frac{T_{0,H=0} - 0.0065H}{T_{0,H=0}}\right)^{5.2552} + \Delta p_{std}. \tag{3}$$

Air intake must be separately modelled in two different assessment groups depending on flight Mach number. As subsonic speed range is considered, a conventional air intake is modelled, up to a maximum of $M_0 = 0.95$, which is the ultimate velocity reached by subsonic aircraft. The diffuser duct has a moderate deceleration; thus, the optimum operating condition is set to $M_0 = 0.6$, at which the ram recovery reaches a peak, in all other conditions this parameter decreases according to a nonlinear law of Mach number, as described in Eq. (4):

$$\sigma_{intake} = \frac{p_{t2}}{p_{t0}} = 0.97 - 0.03\left|0.6 - M_0\right|^{1.35}. \tag{4}$$

2.2 Compressor model

Instead of a complete mathematical model based on physical laws, this model uses a simplified concept that focuses on the cooperation of the three major parts of the engine: compressor, turbine, and nozzle. The engine is equipped with a fixed jet pipe, thus, the cooperation of the above-mentioned components degrades to a single curve on the compressor characteristic map, as seen in Fig. 2. The curve has been determined by measurements and is superposed over the factory map of the compressor under investigation.

Thus, instead of calculating all aspects of the compressor by aero-thermodynamic correlations, the following simplified equations are integrated into the model.

In order to investigate the behaviour of TPR in case of engine deterioration, the authors chose to implement a baseline compressor model and a deteriorated one based on the results disseminated in a conference paper by (Meher-Homji et al., 2013). These changes involve pressure ratio, mass flow rate and efficiency on the side of the compressor. It is assumed to have an influence on the turbine inlet temperature as well, which is discussed later. The engine with no deterioration is called as nominal or baseline engine. The authors only included a single point

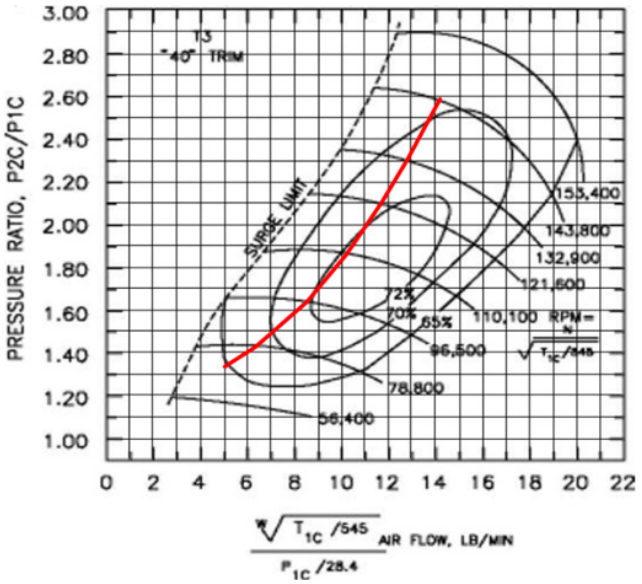

Fig. 2 Compressor map showing cooperation curve of engine components

of deterioration instead of implementing a complete progress of the degradation. This is considered too complex to be included in a single investigation and will be performed later. The effects of a degradation in the turbine were similarly abandoned, as it will have similar influence on engine output parameters.

2.2.1 Rotor speed

As the compressor used in the particular engine is originally developed by Garrett for turbochargers, rotor speed is normalized with an inlet total temperature, which is typical in piston engines. Original corrected rotor speed is described by the formula seen in Fig. 2 and Eq. (5):

$$n_{corr} = n\sqrt{\frac{T_{t2}(R)}{545\ R}} = n\sqrt{\frac{T_{t2}(\mathrm{K})}{302.78\ \mathrm{K}}}. \tag{5}$$

However, it needs to be modified according to the different station numbering, SI units used here, and standard day correction, as shown in Eq. (6). Note that indexing is simplified to "c" as this parameter will be used in the majority of the model.

$$\begin{aligned} n_c &= n\sqrt{\frac{T_{t2}(\mathrm{K})}{288.15\ \mathrm{K}}} \\ &= n\sqrt{\frac{T_{t2}(\mathrm{K})}{302.78\ \mathrm{K}}}\sqrt{\frac{302.78\ \mathrm{K}}{288.15\ \mathrm{K}}} = 1.025 n_{corr}. \end{aligned} \tag{6}$$

This scaling factor will be incorporated into the model when transforming physical rotor speed to corrected one, as the model calculates in SI and standard day conditions,

meanwhile the original map contains factory correction data. Thus, the maximum value of 153,400 RPM corresponds to a physical speed of n_{nom} = 149,609 RPM under standard atmospheric conditions, hence, this value will be used throughout the investigation as the nominal rotor speed, all relative values are normalized by this value, as indicated in Eq. (7):

$$\bar{n}_c = \frac{n_c}{n_{nom}}. \tag{7}$$

2.2.2 Mass flow rate

Similar to the rotor speed, mass flow must be normalized in a different way in contrast to that used by the manufacturer, including a common depression in the intake duct of a piston engine, as shown in Fig. 2 and Eq. (8):

$$\begin{aligned}\dot{m}_{corr} &= \dot{m}\left(\frac{lb}{\min}\right)\frac{28.4\ inHg}{p_{t2}(inHg)}\sqrt{\frac{T_{t2}(R)}{545\ R}} \\ &= \dot{m}\left(\frac{lb}{\min}\right)\frac{96173\ \text{Pa}}{p_{t2}(\text{Pa})}\sqrt{\frac{T_{t2}(\text{K})}{302.78\ \text{K}}}.\end{aligned} \tag{8}$$

The problem of Eq. (8) is not only the usage of non-standard correction factors and units, but also that it is not a non-dimensional ratio. It is more suitable for the present model to include the non-dimensional mass flow rate, $q(\lambda)$, indicated in Eq. (9):

$$\begin{aligned}q(\lambda) &= \frac{\dot{m}\sqrt{T_{2t}}}{p_{t2}A_2\beta_{air}} \\ &= \underbrace{\dot{m}\left(\frac{lb}{\min}\right)\frac{96173}{p_{t2}}\sqrt{\frac{T_{t2}}{302.78}}}_{\dot{m}_{corr}} \\ &\times \underbrace{\frac{1\min}{60\ \text{s}}\times\frac{0.4536\ \text{kg}}{1\ lb}\times\frac{\sqrt{302.78}}{96173\times A_2\beta_{air}}}_{K_q}.\end{aligned} \tag{9}$$

In (9), A_2 is the compressor inlet cross-sectional area, which equals to 1.116 × 10^{-3} m^2, β_{air} is a dimensionless constant of various material properties, for pure air it is 0.0404. Thus, the factor between the corrected mass flow rate given by factory data and the non-dimensional mass flow rate $q(\lambda)$ can be determined as seen in Eq. (10):

$$K_q = \frac{1\min}{60\ \text{s}}\times\frac{0.4536\ \text{kg}}{1\ lb}\times\frac{\sqrt{302.78}}{96173\times A_2\beta_{air}} = 0.03034. \tag{10}$$

Thus, one can rescale the horizontal axis of Fig. 2, from where the dimensionless mass flow rate can be plotted against corrected rotor speed as shown with blue markings in Fig. 3 and its Eq. (11) can be determined. Note that the deteriorated points are also plotted with red color in Fig. 3.

$$q(\lambda)_n = -0.0893(\bar{n}_c)^2 + 0.6928\bar{n}_c - 0.142. \tag{11}$$

This correlation will be used when dimensionless mass flow rate must be determined after relative corrected rotor speed has been established. Afterwards, the physical mass flow rate is found from Eq. (12):

$$\dot{m} = \frac{q(\lambda)p_{t2}A_2\beta_{air}}{\sqrt{T_{t2}}}. \tag{12}$$

In case of degradation, the assumption is that the damage is of 1% efficiency drop, which in turn results in a 1.2% decrease in mass flow rate according to the model discussed by (Meher-Homji et al., 2013). Thus, the changed equation is indicated in Eq. (13):

$$q(\lambda)_d = -0.1032(\bar{n}_c)^2 + 0.716\bar{n}_c - 0.1713. \tag{13}$$

2.2.3 Pressure ratio

In contrast to the two previously detailed parameters, pressure ratio does not have to be rescaled, and can be used in the model immediately. Forming pairs of rotor speed and pressure ratio values from the points of the cooperation curve in Fig. 2, the following function can be determined, as depicted in Fig. 4, and shown in Eq. (14):

$$\pi_c = 2.6409(\bar{n}_c)^2 - 1.1254\bar{n}_c + 1.3104. \tag{14}$$

Equation (14) will be used when pressure must be determined after relative corrected rotor speed has been established. Thus, using Eq. (15) compressor outlet total pressure can be calculated:

$$p_{t3} = p_{t2}\pi_c. \tag{15}$$

In case of deteriorated compressor, Eq. (14) is modified according to (Meher-Homji et al., 2013). Their investigation showed an approximate 1.08% reduction in

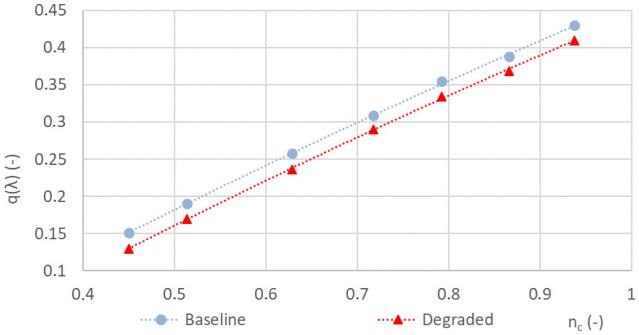

Fig. 3 Change of dimensionless mass flow rate $q(\lambda)$ as a function of relative standard day corrected rotor speed $\bar{n}_c$

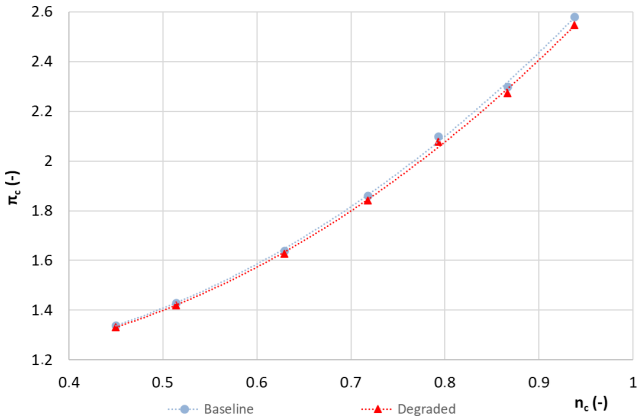

Fig. 4 Change of compressor pressure ratio π_c as a function of relative standard day corrected rotor speed $\bar{n}_c$

compressor pressure rise; this was converted into pressure ratio as shown in Eq. (16):

$$\pi_{c,d} = 2.6409\left(\bar{n}_c\right)^2 - 1.1254\bar{n}_c + 1.3104. \tag{16}$$

2.2.4 Efficiency

Regarding the isentropic efficiency of the compressor, the values were interpolated from Fig. 2 and the relationship shown in Eq. (17) and Fig. 5 has been determined. Thus, the compressor temperature rise can be calculated as shown in Eq. (18):

$$\eta_c = -0.8698\left(\bar{n}_c\right)^2 + 1.2792\bar{n}_c + 0.248, \tag{17}$$

$$\Delta T_c = T_{t2}\frac{\left(\pi_c^{\frac{\kappa_a - 1}{\kappa_a}} - 1\right)}{\eta_c}. \tag{18}$$

In Eq. (17), κa is the adiabatic exponent of the air in the temperature range of (T_{t2}, T_{t3}). Because the compressor temperature rise implicitly depends on this parameter, the calculation requires iteration with an assumed initial temperature, until it yields an acceptable convergence.

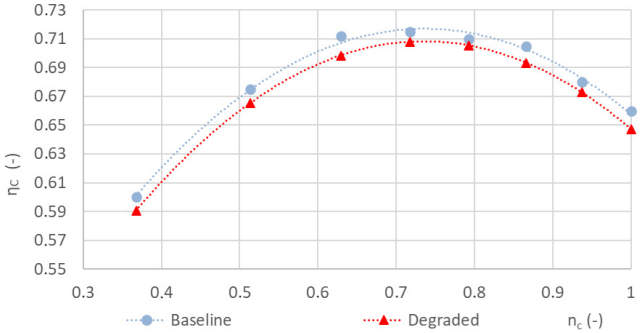

Fig. 5 Change of compressor isentropic efficiency η_c as a function of relative standard day corrected rotor speed $\bar{n}_c$

Thus, the stagnation temperature at the compressor discharge can be expressed as shown in Eq. (19):

$$T_{t3} = T_{t2} + \Delta T_c. \tag{19}$$

The assumption about efficiency drop in the deterioration is that the effect is uniform over the entire speed range, thus the shape of the curve does not change, only the offset value is modified. Thus, the same Eq. (17) can be used, only the last coefficient shall be changed to 0.238, one hundredth lower than in the undeteriorated case.

2.3 Combustor model

This component is responsible for generating heat energy from the chemical bonds of the fuel and oxygen. The most important parameters are stagnation pressure recovery factor σ_{cc} and combustor outlet temperature T_{t4}. The former is assumed to have a constant value of 0.95 throughout the entire operating range. As the stagnation pressure recovery factor is known turbine inlet total pressure can be calculated according to Eq. (20):

$$p_{t4} = p_{t3}\sigma_{cc}. \tag{20}$$

Combustor outlet temperature is normalized using results of an earlier measurement. Fig. 6 shows the measured values as discrete points as a function of standard day corrected rotor speed, along with a second-order polynomial estimation, whose relationship is given in Eq. (21):

$$T_{t4,c} = T_{t4}\frac{288}{T_{t2}} = 2311.8\left(\bar{n}_c\right)^2 - 2607.4\bar{n}_c + 1644.3. \tag{21}$$

The deterioration is assumed to have a step increase of five Kelvins in turbine inlet temperature in contrast to the baseline model shown in Eq. (21).

The previous calculation results in a normalized turbine inlet temperature value, but the turbine itself operates

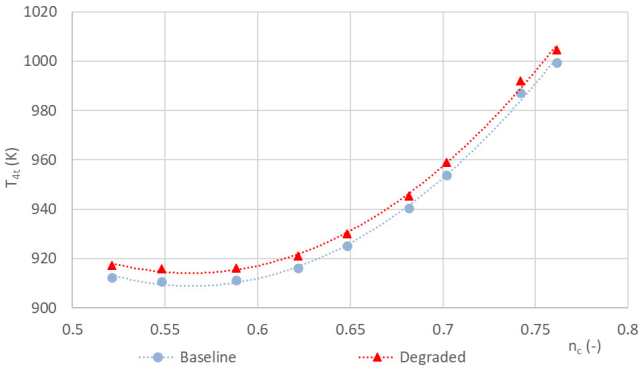

Fig. 6 Change of turbine inlet stagnation temperature T_{t4} as a function of relative standard day corrected rotor speed $\bar{n}_c$

with real physical values, which can be obtained by rearranging Eq. (21) according to Eq. (22):

$$T_{t4} = T_{t4,corr} \frac{T_{t2}}{288}. \tag{22}$$

Fuel mass flow rate is not calculated in this model, as it is not required by other processes. Therefore, an average value of fuel-to-air ratio is taken into account, $q_T = 0.015$, which corresponds to an intermediate fuel mass flow rate at around 120,000 rpm.

2.4 Turbine model

As the investigation focuses on steady state operation of the turbojet engine, this condition results in an equilibrium of power demand of the compressor and the power supply of turbine. Supposing there are no offtakes (air from compressor, mechanical power from the shaft), and neglecting the amount of fuel injected, the mass flow rate of the compressor equals to the one measured in the turbine. Thus, one can deduct the power equilibrium to an equity of the mechanical works of the two units. Considering adiabatic operation of both components, work can be expressed as the product of isobaric specific heat and temperature rise or drop, respectively. Thus, temperature drop of turbine can be calculated from the temperature rise of the compressor scaled by the ratio of the two isobaric specific heats of the two units, as shown in Eq. (23):

$$c_{p,air}\Delta T_c = c_{p,gas}\Delta T_t \rightarrow \Delta T_t = \frac{c_{p,air}}{c_{p,gas}}\Delta T_c. \tag{23}$$

2.5 Exhaust nozzle model and thrust output

The model incorporates a description of a fixed area nozzle, which is typical in subsonic applications. This will strongly influence how the regimes must be handled in which the nozzle pressure ratio surpasses the critical one.

After turbine discharge pressure is obtained, the remaining pressure ratio available for nozzle expansion can be determined as shown in Eq. (24), taking into account losses in the diffuser downstream of the turbine, which is approximated as a constant recovery factor of $\sigma_D = 0.98$:

$$\pi_N = \frac{\sigma_D \times p_{t5}}{p_0}. \tag{24}$$

As the pressure ratio across the exhaust nozzle is known, the velocity of exhaust gasses can be obtained as indicated in Eq. (25) by one of two simple gas dynamic correlations depending on whether the pressure ratio surpasses the critical one or not. Furthermore, an efficiency of $\eta_N = 0.96$ is assumed for the expansion process throughout the exhaust nozzle.

$$c_8 = \begin{cases} \sqrt{\frac{2\kappa_N}{\kappa_N - 1} RT_{t5}\left(1 - \pi_N^{\frac{\kappa_N - 1}{\kappa_N}}\right)\eta_N} & \text{if } \pi_N < \pi_{crit} \\ \sqrt{\frac{2\kappa_N}{\kappa_N + 1} RT_{t5}\eta_N} & \text{if } \pi_N \geq \pi_{crit} \end{cases}. \tag{25}$$

In Eq. (24), κ_N is the mean adiabatic exponent of the gas passing through the exhaust nozzle, between temperatures T_{t5} turbine discharge total and T_8 nozzle exit static ones. This requires an additional iteration until an accurate value of T_8 is obtained. On the other hand, R is the specific gas constant, which depends only slightly on the actual composition of the exhaust gas; therefore, it is assumed to have a fixed value $R = 288$ J/(kg K).

The next step is to determine whether the outlet static pressure is larger than the ambient one or not:

$$p_8 = \begin{cases} p_0 \text{ if } \pi_N < \pi_{crit} \\ \frac{\sigma_D p_{t5}}{\pi_{crit}} \text{ if } \pi_N \geq \pi_{crit} \end{cases}. \tag{26}$$

Now the thrust output of the engine can be calculated with the expression in Eq. (27):

$$F = \begin{cases} \dot{m}\left(c_8 - v_0\right) \text{ if } \pi_N < \pi_{crit} \\ \dot{m}\left(c_8 - v_0\right) + A_8\left(p_8 - p_0\right) \text{ if } \pi_N \geq \pi_{crit} \end{cases}. \tag{27}$$

Relative thrust is obtained by dividing the actual value with the one that belongs to the sea level standard conditions as indicated in Eq. (28):

$$\bar{F} = \frac{F_{act}}{F_{nom}}. \tag{28}$$

Furthermore, a corrected relative thrust is calculated, which is the ratio of the actual relative thrust and actual static ambient pressure, which is the thrust generated by the engine at the same operating regime under different ambient pressure conditions, as seen in Eq. (29). In the majority of the cases, the corrected relative thrust will be used as a basis.

$$\bar{F}_c = \frac{\bar{F}}{p_0} \tag{29}$$

3 Investigations performed with the mathematical model of the turbojet engine

3.1 Verification of the model

The initial assessment was performed with a constant physical rotor speed, which produced such diagrams that

can be compared to data given in literature, to verify the correct operation of the model.

As depicted in Fig. 7, the curves of relative thrust at different flight altitudes completely match the awaited performance, thus, the model can be considered as validated. The altitudes range from sea level to 11 km with steps basically equal to 3 km, except for the last one, where 2 km is the difference to match the standard upper limit of the troposphere. These altitude values will be used throughout the entire investigation with different aspects as well. Fig. 7 represents two sets of curves; in each set one can find a curve that belongs to the nominal operational condition and another one which depicts the circumstances of degraded compressor. The values for the latter curves are indicated with the index "*d*".

The data shown in Fig. 7 verifies the expectation that thrust is decreasing when climbing to higher altitudes, meanwhile the physical rotor speed is constant. The Mach effects are also evident, as the thrust begins to drop in contrast to its static value first in the low Mach number region, then it turns into an accelerating rise surpassing the static thrust itself at around 0.4 Mach. Meanwhile, TPR shows an initially slow then rapidly decreasing function, which is offset towards higher values when altitude is increased. This is natural, as the gas turbine operated at constant physical speed experiences increasing corrected speed due to the reduction in ambient temperature. Thus, the unit works as if it would be accelerated under sea level conditions; this explains why the thrust parameter TPR increases with altitude under this circumstance.

Another important aspect should be investigated, namely, how the relative corrected thrust changes in this case. The results can be seen in Fig. 8, evidently showing both relative corrected thrust and relative corrected rotor speed curves are offset in the increasing direction due to the previously mentioned effect. It is important to note that Fig. 8 does not include different curves for normal and degraded conditions regarding the relative corrected speed. The reason is that the assumption of constant physical rotor speed results in exactly the same corrected speeds when the ambient conditions match. Thus, a single curve represents both conditions for relative corrected speeds at any altitude.

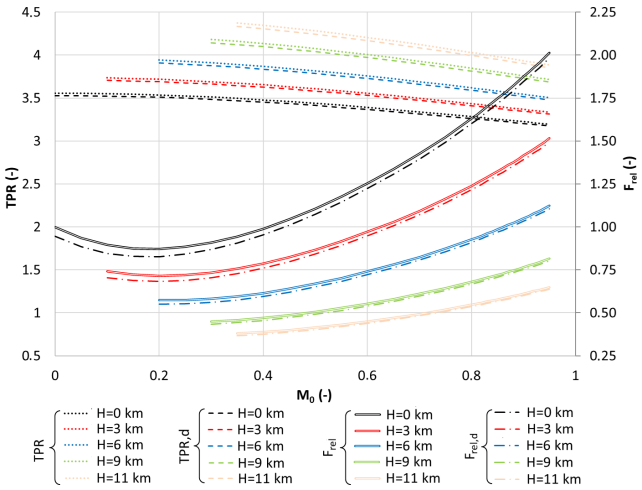

Fig. 7 TPR and relative thrust curves for nominal and deteriorated engine at different flight altitudes as a function of Mach number of flight with physical rotor speed *n* maintained at constant value

3.2 Investigation of modification function to maintain constant corrected thrust output

After the validation, the change of relative thrust is investigated with either standard day corrected rotor speed or TPR held at a constant value. It is evident that, due to Mach effects, the corrected thrust changes even if the given thrust parameter is maintained. Therefore, the main goal of this part of the investigation was to establish a function for TPR, to which the originally constant value must be modulated in order to keep the corrected thrust output at a desired constant level. The two functions can be seen in Fig. 9.

In case the corrected rotor speed is used as thrust parameter, the modulating factor as a function of Mach number is indicated by the solid lines in Fig. 9. It is evident that a specific corrected rotor speed results in a certain corrected thrust, therefore, in order to cancel Mach effects, the same function will be suitable for all flight altitudes. The equation of the modifier function M_n is shown in Eq. (30), which was derived from a third-order polynomial fit using least

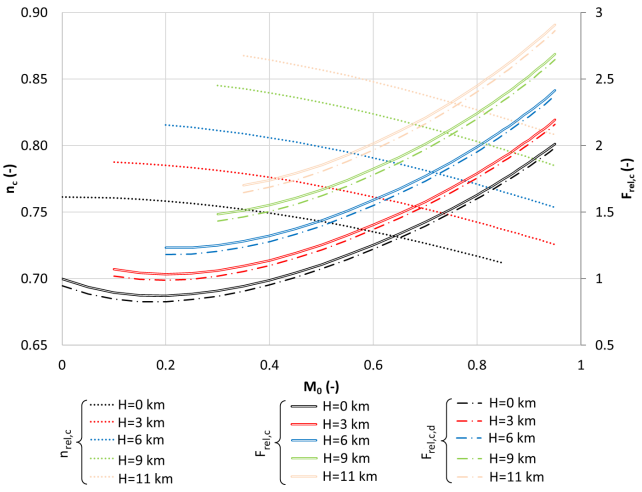

Fig. 8 Corrected rotor speed and relative corrected thrust curves for normal and deteriorated engine at different flight altitudes as a function of Mach number of flight with physical rotor speed *n* maintained at constant value

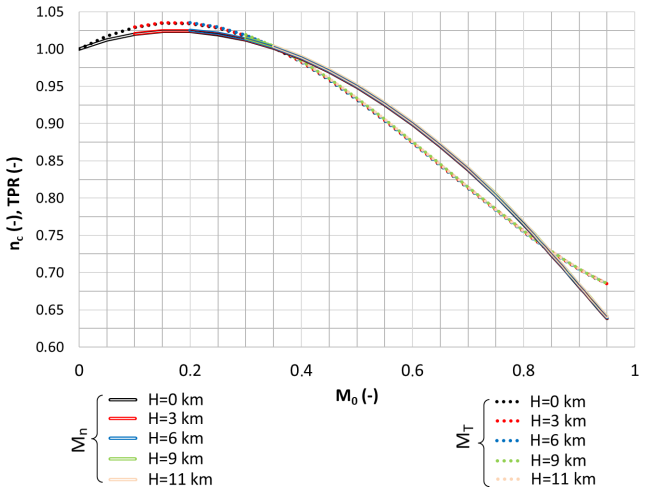

Fig. 9 Corrected rotor speed and TPR functions that allow maintaining of constant corrected thrust as a function of Mach number of flight

squares method on the data, with a restriction that at zero Mach number the value of the function must be unity. Thus, if a control system maintains $M_n \times n_c = const.$, the corrected thrust will remain the same regardless of flight conditions including altitude and speed:

$$M_n = 0.1418 \times Ma^3 - 0.8279 \times Ma^2 + 0.2768 \times Ma + 1. \quad (30)$$

As Fig. 9 shows, it is also evident that TPR correction lines overlap as well. This means that TPR is also useful as thrust parameter, however, its modifier function MT slightly differs from that of corrected rotor speed. This is obtained similarly, and its equation is shown in Eq. (31):

$$M_T = 0.8215 \times Ma^3 - 1.6272 \times Ma^2 + 0.4708 \times Ma + 1. \quad (31)$$

3.3 Investigation of a deteriorated engine behaviour according to corrected rotor speed or TPR control

Based on the work of Rowe and Kurz (1999), the main benefit of using TPR in control system is that it will be able to compensate for deterioration of the power plant. Their focus was on high bypass ratio turbofan engine, therefore, they assessed the effect of fan stage damage as foreign objects surely pass through this part of the gas turbine. In the present survey, the authors similarly chose the frontal section of the turbojet engine, namely the compressor, although there might be damage appearing in the hot section as well, but the likelihood of compressor fouling, or other deterioration is higher.

The two conditions, which were compared, are the deteriorated engine with rotor speed control and behaviour of the engine with the same deterioration controlled by TPR. In each case, the reference was the undamaged engine performance.

In Fig. 10, one can see the deviation in both cases as a relative change in thrust output and the difference how many percent thrust is gained back using TPR control over rotor speed regulation.

It is evident that TPR regulation provides a noticeable gain in thrust, even if it will not provide exactly the same output as the undamaged engine. This gain has a peak in the low Mach number range, its amplitude diminishes with increasing flight altitude. The Mach number at which the peak occurs slightly increases when the aircraft climbs. The gain reduces when reaching large cruise Mach numbers, but it still remains positive, ensuring superiority of the TPR control over the entire subsonic range.

It is also visible in Fig. 10, that TPR control provides less than 1% loss in thrust despite the engine damage from an average 0.45 Mach number (nearly 0.4 at high altitudes and 0.5 at sea level); meanwhile the average loss of thrust with rotor speed control was around 2.2% in the upper Mach number range. This fact emphasizes the benefits of TPR control when the engine deteriorates from its nominal condition due to damage.

4 Discussion

The model supplied such verification results, which were in line with the expectations. Therefore, the authors have conducted the two other parts of the investigation, namely the establishment of a modifier function to maintain constant corrected thrust and the investigation of the behaviour of TPR control with deteriorated engine hardware.

4.1 Discussion of modifier functions

Regarding the establishment of the modifier function for TPR control, another evidence was shown that TPR is

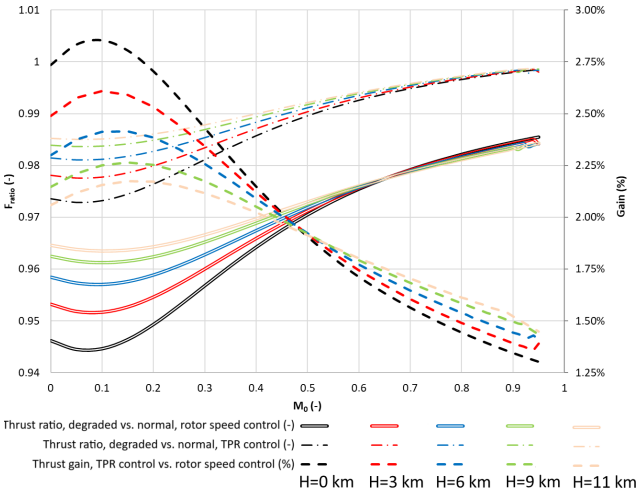

Fig. 10 Change in thrust output of the deteriorated engine as a percentage of the nominal thrust for rotor speed and TPR control

suitable for turbojet engines' thrust parameter, because in case of constant TPR the turbojet develops the same corrected thrust output. It is an interesting fact that TPR is thus proportional to the corrected value instead of the physical one. Nevertheless, it is known from gas dynamics and similitude theory that, due to changing ambient conditions, the physical values of thrust will differ (e.g., in sea level application and in cruise) even if the engine itself is running in the same operational mode. That is why thrust is normalized by the ambient pressure, as this method ensures that the resulting corrected values will match whenever the engine performs at the same operational mode.

It is an interesting result of this investigation that the modifier function for the TPR crosses the curve for corrected rotor speed modifier three times throughout the subsonic range, as seen in Fig. 9. They have a nodal point at steady conditions, where both parameters reach their nominal values.

The second nodal point occurs at around 0.35 Mach number. Between zero and this value, TPR modifier surpasses the one for corrected rotor speed, because TPR decay is more emphasized in this speed range as seen in Figs. 7 and 8, and reaches around 10% decrement while rotor speed droops only by 5% in the same range. Therefore, TPR modifier first must be higher than the corresponding values of corrected rotor speed modifiers.

Until approximately 0.85 Mach number, the TPR modifier runs below the corrected speed modifier function, at which point they establish a third nodal point.

4.2 Discussion of effects of deterioration

When the engine damage leads to less effective operation of the components, these effects will accumulate and result in a much larger loss in thrust output than could be predicted from the individual efficiency decrease. This can lead to a 5.5% loss in output at sea level conditions with low Mach numbers. Although the amplitude surely diminishes as the aircraft climbs to higher altitudes, the reduction in thrust should be accommodated somehow.

If the engine is controlled by TPR, Fig. 10 shows evidently that thrust output is always higher than the corresponding value with corrected rotor speed control. There is not any combination of Mach number and flight altitude, which would result in a less powerful operational mode of TPR control. That is why engine control system designers may choose TPR as primary control, or, if they rely mostly on conventional corrected rotor speed algorithms, TPR can be a backup mode of operation only activated when deteriorations are already present in the system. Whichever is the decision, engine reliability and performance can be improved together, which surely leads to noticeable increase in useful service life of the engines.

4.3 Discussion of further diagnostic capabilities of TPR

Another interesting consequence of the usage of TPR is the possibility of comparison of nominal ratios against other commonly measured engine performance parameters. As an example, the ratio of TPR versus normalized corrected rotor speed is depicted in Fig. 11 as a function of Mach number, for the previously investigated altitudes.

In Fig. 11, one can see that TPR-to-speed ratio slightly decreases as Mach number rises: by 2.3 to 4.7% of the value at the minimum Mach number of that particular altitude. The lower value belongs to the sea level conditions, and as altitude increases, so does the slope of the curve.

Regarding the dashed curves in Fig. 11, it is evident that TPR (as a thrust parameter) reduces as compared to the corrected rotor speed. If the diagnostic system continuously monitors this ratio, it can have a determined threshold at which it gives warning to the crew about impending engine malfunction.

As the present investigation only involved a single estimate of a particular deterioration level besides the baseline engine configuration, the amount of data available is not enough to determine a correlation between deterioration

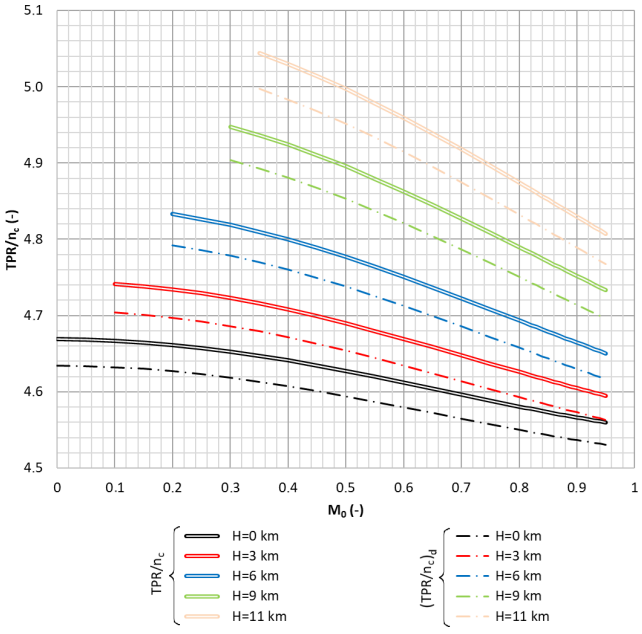

Fig. 11 TPR versus normalized corrected rotor speed ratio over the investigated Mach number and altitude range, with baseline and deteriorated engine

level and TPR-to-speed ratio. However, the authors suggest that the establishment of such a function that results in a numerically expressed health condition of the engine shall be performed in the following way.

First, a more detailed deterioration model must be implemented that allows the investigation of multiple levels of the process. The deterioration level should be defined as a real number which expresses the reduction of thrust output in one tenth percent of the nominal thrust, i.e., in case of 1% loss the health parameter would be equal to ten. This allows the crew to monitor the process with enough accuracy but still may remain simple. Then, the system should continuously monitor the necessary engine signals creating the above-mentioned health parameter. The health parameter should be recorded together with the time of measurement in order to provide not only an instantaneous value of the actual condition but also offer the overview of the trend and give the possibility of prognosis based on historical data. This way, in case the health parameter or its time derivative reaches one of more (e.g., two) predetermined thresholds (like early warning and alert levels), the diagnostic system can generate different associated alerts for the crew (either maintenance or flight crew). Thus, the system can warn the operator before a catastrophic failure occurs, significantly reducing the costs of repair and loss of profit due to aircraft on ground.

5 Conclusion

The authors established a simplified mathematical model of a turbojet with most nonlinear effects taken into account and performed various investigations using this model.

During the assessments, the authors have determined the modifier function that shall be used in conjunction with the TPR control to modulate the TPR reference value under changing Mach number conditions to maintain a stable, constant corrected thrust output of the turbojet engine.

The authors have also focused on the diagnostic capabilities of the TPR parameter and showed that this variable offers an additional benefit when the engine deteriorates from its nominal conditions due to damage in its hardware. This benefit manifests in thrust gain, as TPR control of a deteriorated engine can produce much closer thrust outputs to the nominal values despite the deterioration, which is already present in the engine.

In order to establish an engine health parameter that can describe the magnitude of the deterioration, based on measurements of the nominal engine, a cross-reference table should be established between corrected rotor speed and TPR as a function of Mach number and flight altitude. Thus, the control system can permanently monitor the performance of the engine and can take accommodation strategies if necessary. Either TPR control is selected all the times and this will automatically prevent the loss of thrust due to deterioration, or TPR control can be selected over the normal corrected rotor speed algorithm in case of notable deviation from the nominal speed versus TPR schedule.

It was also introduced how TPR-to-speed ratio can be used in advanced diagnostic systems, which improves the reliability of the power plant, can cut costs of maintenance by offering early warning and an exact numerically expressed level of the engine deterioration.

The investigation was carried out for a subsonic configuration with an air intake having round lip and a fixed nozzle. In the future, the assessment should be repeated with a slightly modified model that allows to take into account the effect of an air intake and a variable nozzle, and thus the speed range can be extended into supersonic velocities.

Another possible improvement of the present assessment could be the introduction of a detailed calculation of fuel supply instead of a constant fuel-air ratio.

Furthermore, an important development will be the implementation of a thoroughly elaborated model of deterioration to determine the exact TPR-to-speed ratio under any arbitrary degradation level, which can be then used to notify crew about impending engine malfunction.

As a final conclusion, it is evident that using TPR instead of corrected rotor speed will have several benefits and therefore such a control system can help coping with engine deterioration, which never can be cancelled in real operating conditions.

References

Andoga, R., Főző, L., Schrötter, M., Češkovič, M., Szabo, S., Bréda, R., Schreiner, M. (2019) "Intelligent Thermal Imaging-Based Diagnostics of Turbojet Engines", Applied Sciences, 9(11), 2253. https://doi.org/10.3390/app9112253

Andoga, R., Főző, L., Schrötter, M., Szabo, S. (2021) "The Use of Ethanol as an Alternative Fuel for Small Turbojet Engines", Sustainability, 13(5), 2541. https://doi.org/10.3390/su13052541

Arif, I., Masud, J., Shah, S. (2018) "Computational Analysis of Integrated Engine Exhaust Nozzle on a Supersonic Fighter Aircraft", Journal of Applied Fluid Mechanics, 11(6), pp. 1511–1520. https://doi.org/10.29252/jafm.11.06.28989

Aygun, H., Kirmizi, M., Kilic, U., Turan, O. (2023) "Multi-objective optimization of a small turbojet engine energetic performance", Energy, 271, 126983. https://doi.org/10.1016/j.energy.2023.126983

Balli, O. (2022) "A Parametric Study of Hydrogen Fuel Effects on Exergetic, Exergoeconomic and Exergoenvironmental Cost Performances of an Aircraft Turbojet Engine", International Journal of Turbo & Jet-Engines, 39(4), pp. 477–490. https://doi.org/10.1515/tjj-2019-0043

Balli, O., Kale, U., Rohács, D., Karakoc, T. H. (2022) "Exergoenvironmental, environmental impact and damage cost analyses of a micro turbojet engine (m-TJE)", Energy Reports, 8, pp. 9828–9845. https://doi.org/10.1016/j.egyr.2022.07.157

Beneda, K. (2015) "Modular Electronic Turbojet Control System Based on TPR", Acta Avionica, 17(1), pp. 1–14. [online] Available at: https://acta-avionica.tuke.sk/ojs/index.php/aavionica/article/view/893/891 [Accessed: 26 May 2024]

Brodzik, Ł. (2024) "Gas Temperature Distribution in the Combustion Chamber of a GTM400 MOD Turbojet Engine Powered by JET A-1 Fuel and Hydrogen", Energies, 17(3), 745. https://doi.org/10.3390/en17030745

Cican, G., Gall, M., Bogoi, A., Deaconu, M., Crunțeanu, D. E. (2023) "Experimental Investigation of a Micro Turbojet Engine Chevrons Nozzle by Means of the Schlieren Technique", Inventions, 8(6), 145. https://doi.org/10.3390/inventions8060145

Ciupek, B. J., Brodzik, Ł., Semkło, Ł., Prokopowicz, W., Sielicki, P. W. (2024) "Analysis of the Environmental Parameters of the GTM 400 Turbojet Engine During the Co-Combustion of JET A-1 Jet Oil with Hydrogen", Journal of Ecological Engineering, 25(3), pp. 205–211. https://doi.org/10.12911/22998993/178533

Davies, C., Holt, J. E., Griffin, I. A. (2006) "Benefits of inverse model control of Rolls-Royce civil gas turbines", In: Proceedings of UKACC International Control Conference, Glasgow, UK, pp. 70–76. ISBN 0947649549

Derbel, K., Beneda, K. (2019) "Linear Dynamic Mathematical Model and Identification of Micro Turbojet Engine for Turbofan Power Ratio Control", Aviation, 23(2), pp. 54–64. https://doi.org/10.3846/aviation.2019.11653

Derbel, K., Beneda, K. (2020) "Sliding Mode Control for Micro Turbojet Engine Using Turbofan Power Ratio as Control Law", Energies, 13(18), 4841. https://doi.org/10.3390/en13184841

Főző, L., Andoga, R. (2022) "Advanced Control of an Electric Fuel-Oil Pump for Small Turbojet Engines", Aerospace, 9(10), 607. https://doi.org/10.3390/aerospace9100607

Főző, L., Andoga, R., Schreiner, M., Beneda, K., Hovanec, M., Korba, P. (2019) "Simulation aspects of adaptive control design for small turbojet engines", In: 2019 IEEE 23rd International Conference on Intelligent Engineering Systems (INES), Gödöllő, Hungary, pp. 000101–000106. ISBN 978-1-7281-1214-5 https://doi.org/10.1109/INES46365.2019.9109503

Gao, Q., Li, J., Zhang, Y. (2024) "Self-tuning speed and flow control of micro turbojet engines based on an improved evolutionary strategy", Automatika: Journal for Control, Measurement, Electronics, Computing and Communications, 65(3), pp. 1154–1162. https://doi.org/10.1080/00051144.2024.2349869

Ghahramani, Z., Zareh, M., Pourfarzaneh, H., Pazooki, F. (2023) "Optimization the TIT profile in an annular combustion of a turbojet engine based on smart modeling and CFD simulation", Journal of the Taiwan Institute of Chemical Engineers, 148, 104812. https://doi.org/10.1016/j.jtice.2023.104812

Han, D.-J. (2023) "Fault Diagnosis and Its Applications to Fault Tolerant Control of a Turbojet Engine", Energies, 16(8), 3317. https://doi.org/10.3390/en16083317

Meher-Homji, C., F. Bromley, A., Stalder, J.-P. (2013) "Gas Turbine Performance Deterioration and Compressor Washing", In: Proceedings of the 2nd Middle East Turbomachiery Symposium, Doha, Qatar, pp. 1–43. [online] Available at: https://turbolab.tamu.edu/wp-content/uploads/2018/08/METS2Tutorial5.pdf [Accessed: 26 May 2024]

Montazeri-Gh, M., Dastjerdi, A. Y. (2024) "Modeling and experimental analysis of the metering performance of a turbojet engine fuel control unit at start-up regime", Flow Measurement and Instrumentation, 95, 102492. https://doi.org/10.1016/j.flowmeasinst.2023.102492

Przysowa, R., Majewski, P., Ślęczek, J., Grundas, D., Wachłaczenko, M. (2023) "Health monitoring of the shaft bearings in a micro turbojet based on vibration analysis", Journal of Physics: Conference Series, 2526, 012070. https://doi.org/10.1088/1742-6596/2526/1/012070

Rohacs, D., Yasar, O., Kale, U., Ekici, S., Yalcin, E., Midilli, A., Karakoc, T. H. (2023) "Past and current components-based detailing of particle image velocimetry: A comprehensive review", Heliyon, 9(3), e14404. https://doi.org/10.1016/j.heliyon.2023.e14404

Rowe, A. L., Kurz, N. (1999) "Control System for a Ducted Fan Gas Turbine Engine", London, UK, 5,887,419. [online] Available at: http://patentimages.storage.googleapis.com/pdfs/US5887419.pdf [Accessed: 26 May 2024]

Şen, S. (2023) "The effect of using triple bio-fuel blend with Jet-A on engine performance and emissions in mini-scale turbojet engine", Energy Sources, Part A: Recovery Utilization, and Environmental Effects, 45(2), pp. 4616–4632. https://doi.org/10.1080/15567036.2023.2205826

Tang, W., Wang, L., Gu, J., Gu, Y. (2020) "Single Neural Adaptive PID Control for Small UAV Micro-Turbojet Engine", Sensors, 20(2), 345. https://doi.org/10.3390/s20020345

Xiao, T., He, A., Pei, X., Pan, M., Wang, X., Hu, Z. (2023) "Research on Hydrogen-Fueled Turbojet Engine Control Method Based on Model-Based Design", Processes, 11(12), 3268. https://doi.org/10.3390/pr11123268

Yucer, C. T., Nacakli, Y. (2024) "Effects of using hydrogen on the exergetic and environmental damage performance of an UAV turbojet engine", Proceedings of the Institution of Mechanical Engineers, Part C: Journal of Mechanical Engineering Science, 238(11), pp. 5331–5343. https://doi.org/10.1177/09544062231217609

Zare, F., Veress, Á. (2022) "Novel Closed-Form Equation for Critical Pressure and Optimum Pressure Ratio for Turbojet Engines", International Journal of Turbo & Jet-Engines, 39(4), pp. 451–463. https://doi.org/10.1515/tjj-2019-0039